3ª Reunión Española de Optoelectrónica

3rd Spanish Meeting of Optoelectronics

14 - 16 de Julio

July 14 - 16

2003

Leganés, Madrid

Editado por / Edited by:
José Manuel Sánchez Pena
Carmen Vázquez García

Optoel '03

ISBN: 84-89315-29-9
Depósito Legal: M-31881-2003

Impreso en España
Printed in Spain

Imprime: **2Color, s.l.**
Resina 13-15, nave B-13
28021 Madrid

Holographically edge enhanced imaging system

A. Márquez[1], C. Neipp[1], S. Gallego[2], M. Ortuño[2], A. Beléndez[1] and I. Pascual[2]

[1]Depto. de Física, Ingeniería de Sistemas y Teoría de la Señal, Universidad de Alicante
[2]Departamento Interuniversitario de Óptica, Universidad de Alicante

Tel.: +34-96-5903651; Fax: +34-96-5909750; E-mail: amarquez@dfists.ua.es

Topic of interest: Optical techniques.
Keywords: Bragg diffraction, Edge-enhancement, Photopolymer.

1. Introduction

Edge enhancement is one of the important image processing operations, useful for image enhancement, edge detection, segmentation, etc. In digital image processing edge detection can be realized in either the spatial or the frequency domain [1]. In optical image processing, both spatial domain and frequency domain based methods are available even though the later have been by large mostly reported in literature. Despite their differences, both the 4-f correlator and the joint-transform correlator (JTC) architectures [2] can be considered frequency domain based methods, since a physical Fourier plane can be identified in the system.

In the spatial domain approach the architecture of the optical processor is that of an imaging system where a volume diffraction grating has been inserted [3]. Spatial filtering is achieved with no need of a physical Fourier plane. Bragg diffraction exhibited by volume gratings is the physical phenomenon responsible for image processing. The system is simple and compact, offering distinctive advantages with respect to Fourier processors. Edge detection using this approach has been mainly studied by people working with acousto-optic light modulators (AOLMs) [4-6], where a programmable volume grating is generated. If programmability is not the main issue, then holography offers a natural and inexpensive procedure to produce high quality volume gratings [7]. Recently, we demonstrated the application of a holographically recorded volume phase grating generated on a PVA/acrylamide photopolymer to edge enhancement [8].

We want to stress the application of holographically recorded volume gratings to edge enhancement in an imaging system. In this work, we focus on the analysis of certain properties offered by Bragg diffraction. We give both simulated and experimental results.

2. Theory

Image processing operations by Bragg diffraction are based on the angular selectivity presented by the zero and the first diffracted orders by volume gratings. In general, whereas the zero (or transmitted) order behaves as a high pass filter, the first (or diffracted) order has the characteristics of a low pass filter.

In AOLMs, Bragg diffraction effects have been described using the frequency transfer function formalism [4,5]. To this goal, we proposed [8] the closed-form expressions from Kogelnik's theory to calculate the frequency transfer functions. We proved that they provide an accurate description for the spatial filtering operations performed by holographic gratings. According to Kogelnik's theory [9], for a volume phase unslanted transmission grating the expressions for the transmitted R and the diffracted S wave amplitudes after passing through the hologram are,

$$R = \exp(-j\xi)\left(\cos\sqrt{\nu^2+\xi^2} + j\xi\, sinc\sqrt{\nu^2+\xi^2}\right) \quad (1)$$

$$S = \exp(-j\xi)(-j\nu)sinc\sqrt{\nu^2+\xi^2} \quad (2)$$

where $sinc(x) = sin(x)/x$ and,

$$\nu = \frac{\pi\,\Delta n\, d}{\lambda_0 \cos\theta_r'};\ \xi = \frac{\pi d}{\Lambda\cos\theta'_r}\left(|sin\theta'_r| - \frac{\lambda_0}{2n_0\Lambda}\right) \quad (3)$$

n_0 and Δn are respectively the average and the modulation of the refractive index, d is the thickness of the medium, Λ is the period of the grating, λ_0 is the wavelength of reconstruction in air and θ_r' is the angle of reconstruction in the recording medium related to the angle of reconstruction in air θ_r by Snell's law. Bragg angle θ'_{Bragg} inside the material is given by,

$$sin\theta'_{Bragg} = \lambda_0/2n_0\Lambda \quad (4)$$

thus ξ (eq. (3)) expresses deviation from the Bragg condition. The parameter ν expresses the amplitude of the phase modulation recorded in the volume grating.

Wave amplitudes R and S given by eqs. (1) and (2) depend on the angle θ_r of the incident beam with respect to the normal of the hologram. According to Figure 1, let us consider θ_o and ψ respectively as the angles of the plane wave spectrum of an input object and the orientation of the grating with respect to the optical axis in a

certain optical system. Thus the angle θ_r is given by $\theta_r = \theta_o - \psi$, and the angular responses *R* and *S* of the grating modify the spectrum of plane waves propagating from the object. Similarly, equations (1) and (2) can be expressed as a function of the angular frequency *p* (rad/meter), given by $p = 2\pi \sin\theta_o / \lambda_0$, to obtain the angular frequency transfer functions $H_0(p)$ and $H_1(p)$ for the zero and the first diffracted orders.

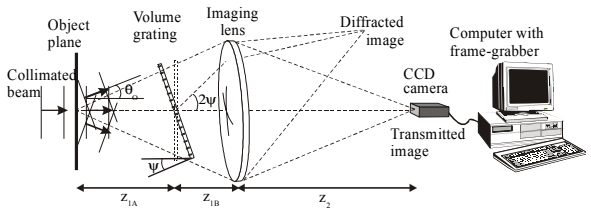

Figure 1. Imaging system with a volume grating. We show the deviation of the transmitted and the diffracted images by the grating.

Interesting properties arise when the grating is oriented at $\psi = \theta_{Bragg}$ [6], where θ_{Bragg} is the Bragg angle in air. The essential characteristics of $H_0(p)$ and $H_1(p)$ can be understood if a more simple expression is derived for small angles of incidence $\xi^2 << \nu^2$. We concentrate on the zero order transfer function $H_0(p)$, whose simplified expression becomes,

$$H_0(p) = A + jBp \tag{5}$$

with $A = \cos\nu$ and $B = (Q \Lambda \, sinc\nu)/(4\pi)$. Q is the Klein-Cook parameter expressing the magnitude of the volume effects [7], given by

$$Q = (2\pi\lambda_0 d)/n_0\Lambda^2 \tag{6}$$

In equation (5) the first term does not depend on the incident frequency *p*, while the second term corresponds to a first derivative filter. If $\nu = \pi/2$ then A is zero, and $H_0(p)$ becomes a pure first derivative filter. In the case of AOLMs Davis et al. [6] showed that by changing the amplitude of the sound wave, which is equivalent to a change in ν, it is possible to select the edges to be enhanced and the degree of enhancement.

3. Properties of "Bragg filters"

Next we discuss some simulations where we analyse different properties provided by volume gratings when used in image processing. Specifically we consider unslanted volume phase transmission gratings.

For the sake of comparison with the experimental results presented in Section 4, we consider a one-dimensional object, i.e. a slit, with a width of *70 μm*, shown in Figure 2(a). Extension to two dimensions is straightforward. In Figure 2(b) we plot the Fourier transform (modulus) of the object, scaled for illumination with a wavelength λ_0 = *633 nm* (He-Ne laser). The frequency content is plotted as a function of the angle θ_o (in degrees) for the angular spectrum of the object. We observe the *sinc* behavior corresponding to a Fourier transformed rectangle function.

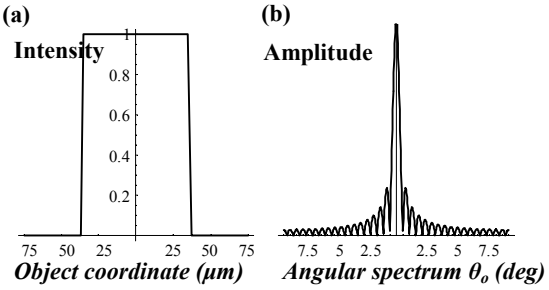

Figure 2. (a) Input object: slit of 70 μm width; (b) Frequency content of the object as a function of the angle θ_o (scaled with λ = 633 nm).

The effect of the grating is characterized by the transfer functions $H_0(p)$ and $H_1(p)$, that we derive from Kogelnik's theory as explained in Section 2. The main parameters that define the profile of the transfer functions $H_0(p)$ and $H_1(p)$ are the Klein-Cook parameter Q, the period Λ of the grating, and the parameter ν:

- Q should be larger than one to be in the Bragg regime.
- A larger product $Q\Lambda$ generates transfer functions with a sharper passband.
- The value of ν allows to select the edge to be enhanced.

To simulate the volume grating we consider the values of the PVA/acrylamide photopolymer that we use in the experiments in Section 4: n_0 = *1.50*, *d* = *88 μm*, Λ = *0.9 μm* (1125 l/mm). For these values, at λ_0 = *633 nm*, we obtain: θ_{Bragg}*(in air)*= ±*20.8°*, Q = *295*, and $Q\Lambda$=*262*.

In Figure 3(a) and 3(c) we show respectively the profiles for the filters $H_0(p)$ and $H_1(p)$ when the grating is oriented at $\psi = \theta_{Bragg}$. Actually we show the modulus as $H_0(p)$ and $H_1(p)$ are complex functions. We consider $\nu = \pi/2$ *rad* (at θ_r = θ_{Bragg}), what means that the grating exhibits 100% diffraction efficiency [7]. Note that the angular interval (X-axis) has been amplified with respect to Figure 2(b). In Fig. 3(b) and 3(d) we show the transmitted and the diffracted images processed respectively by the filters $H_0(p)$ and $H_1(p)$. The transmitted image (Fig. 3(b)) is an edge enhanced version of the input object, and the diffracted image (Fig. 3(d)) is a low pass version where the edges have been smoothed.

If we compare the two images with the input object (Fig. 2(a)) we note that especially the diffracted image (Fig. 3(d)) is clearly shifted from the origin of coordinates. To understand this point let us examine in Figure 4(a) and 4(b) the phase associated respectively with the complex functions $H_0(p)$ and $H_1(p)$. In Figure 4(b) we can see that $H_1(p)$ exhibits a linear phase, what is equivalent to having a prism, thus producing the shift in the position of the diffracted image. Physically, the shifting is due to refraction in the entrance and exit interfaces between air and the medium of the grating [8]. This plane-parallel plate refraction is expressed by the term $\exp(-j\xi)$, which multiplies both eq. (1) and (2). In the case of $H_0(p)$ this shifting is partially compensated by the phase associated with the rest of the terms in equation (2) and we obtain the nonlinear phase profile in Fig. 4(b). This phase profile is responsibles for the asymmetric edge enhancement in Fig. 3(b).

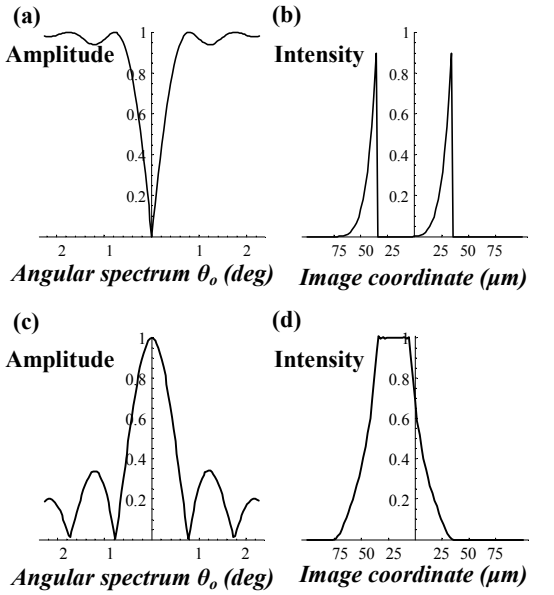

Figure 3. (a) Transfer function (modulus) and (b) image for the zero order. (c) Transfer function (modulus) and (d) image for the first order.

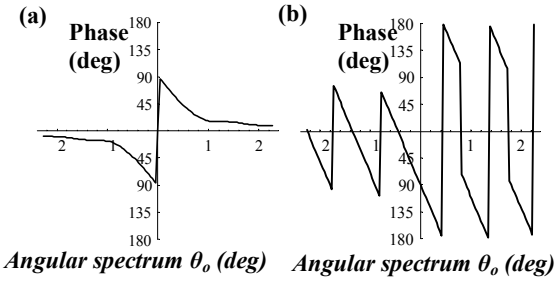

Figure 4. Phase of the (a) zero order transfer function and (b) first order transfer function.

Let us consider that the grating is not oriented at Bragg angle. In Fig. 5(a) and 5(b) we plot respectively the zero order transfer function and the processed image when the grating is *0.5°* out of Bragg incidence. With just *0.5°* of desalignment there is a dramatic change with respect to the image obtained in Fig. 3(b). Thus, any desalignment is clearly visible and can be easily corrected. This would be an advantage of the image processing approach that we are discussing.

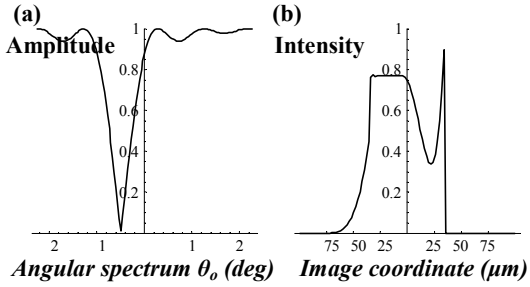

Figure 5. (a) Zero order transfer function (modulus) and (b) transmitted image. The grating is 0.5° out of Bragg incidence.

In Figure 6(a) and 6(b) we plot respectively the zero order transfer function and the transmitted image when $\nu \approx 1.34$ *radians*. The grating is at Bragg incidence $\psi = \theta_{Bragg}$. We observe (Fig. 6(b)) an edge enhanced version of the object where the two edges are not equally enhanced. This is accordance with the calculations in ref. [6], which predict that when $\nu \neq \pi/2$ the degree of enhancement is different for the two edges.

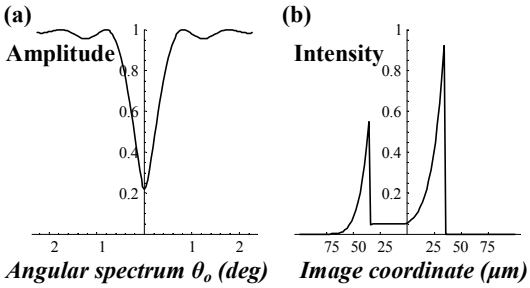

Figure 6. (a) Zero order transfer function (modulus) ($\nu \approx 1.34$) and (b) transmitted image.

4. Experiment

In the experiments a He-Ne laser beam (λ_0 *= 633 nm*) is spatially filtered, expanded, and collimated. The distances in the setup (see Fig. 1) are z_{1A} *= 12 cm,* z_{1B} *= 8 cm,* z_2 *= 59 cm,* the lens has a focal length *f' = 15 cm* and a clear aperture diameter ϕ *= 7.5 cm*, and the magnification of the system is 3. We capture the transmitted (zero order) image using a CCD camera, Hamamatsu C5403, and a frame-grabber, Matrox Meteor, connected to a personal computer.

In the setup we have used an unslanted phase transmission grating recorded on a PVA/acrylamide photopolymer (preparation and composition details in ref. [10]), exposed to the green line (514 nm) of an Argon laser using a symmetrical mount. The two beams form an angle of *16.8°* with respect to the normal of the plate, and generate an interference pattern of *1.5*

cm diameter with a spatial frequency of *1125 lines/mm*. The values for the rest of the parameters of the grating were given in Section 3. In particular $\nu \approx 1.34$ for the grating used in the experiments.

In Fig. 7(a) we see the direct image obtained of the input object by the imaging system when no grating is introduced. The width of the columns composing the number four is approximately *70 μm*, as the object used in the simulations in Section 3. In Figure 7(b) we show the zero order filtered image by the photopolymer grating. We clearly appreciate the edge enhancement produced. The horizontal edges are not enhanced as they are perpendicular to the grating periodicity. We also appreciate that the right edge is slightly brighter than left one. This unequal edge enhancement was also predicted by the simulation in Fig. 6 for $\nu \approx 1.34$.

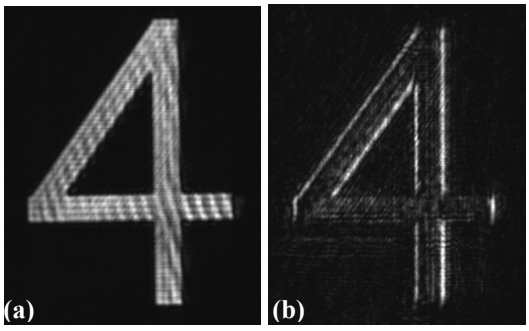

Figure 7. Experimental images. (a) Direct image with no grating; (b) Zero order filtered image.

In Fig. 8 we show the transmitted image of a slit. In Fig. 8(a) the grating is at Bragg incidence and in Fig. 8(b) the grating is 0.5º out of Bragg incidence. We clearly observe that in Fig. 8(b) there is no edge enhancement, as predicted in Fig. 5(b).

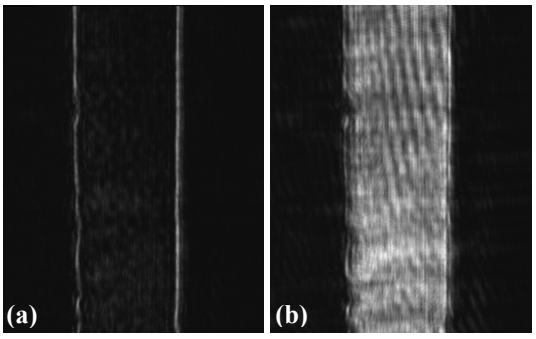

Figure 8. Experimental images for the diffracted order. (a) Grating at Bragg incidence and, (b) Grating 0.5º out of Bragg incidence.

5. Conclusions

We have demonstrated both theoretically and experimental the feasibility of a holographically edge enhanced imaging system. We have analysed the properties of Bragg diffraction when applied to image processing. Analytical expressions have been derived using Kogelnik's theory, which predict the experimental results with a very good agreement. Edge enhancement by Bragg diffraction offers an interesting alternative with respect to Fourier plane based strategies.

Acknowledgments

This work has been partially financed by Ministerio de Ciencia y Tecnología, Spain, project MAT2000-1361-C04-04, and by Generalitat Valenciana, Spain, project GV01-130.

References.

[1] R. C. González and R. E. Woods, *Digital image processing*, (Addison Wesley, New-York, 1993).

[2] J. W. Goodman, Introduction to Fourier Optics, (McGraw-Hill, 2nd edition, New York, 1996)

[3] S. K. Case, "Fourier processing in the object plane", Opt. Lett. 4(9), 286-288 (1979).

[4] J. Xia, D. B. Dunn, T.-C. Poon and P. P. Banerjee, "Image edge enhancement by Bragg diffraction", Opt. Commun. 128, 1-7 (1996).

[5] D. Cao, P. P. Banerjee and T.-C. Poon, "Image edge enhancement with two cascaded acousto-optics cells with contrapropagating sound", Appl. Opt. 37(14), 3007-3014 (1998).

[6] J. A. Davis and M. D. Nowak, "Selective edge enhancement of images with an acousto-optic light modulator", Appl. Opt. 41(23), 4835-4839 (2002).

[7] P. Hariharan, *Optical Holography*, (Cambridge University Press, Cambridge, 1996).

[8] A. Márquez, C. Neipp, S. Gallego, M. Ortuño, A. Beléndez and I. Pascual, are preparing a manuscript with the title "Edge enhanced imaging using PVA/acrylamide photopolymer gratings".

[9] H. Kogelnik, "Coupled wave theory for thick hologram gratings", Bell Syst. Technol. J. 48(9), 2909-2947 (1969).

[10] S. Gallego, M. Ortuño, C. Neipp, C. García, A. Beléndez and I. Pascual, "Overmodulation effects in volume holograms recorded on photopolymers", Opt. Commun.215, 263-269 (2002).